Rheumatology International (2019) 39:2111–2118
https://doi.org/10.1007/s00296-019-04425-2

Rheumatology
INTERNATIONAL

IMAGING

Computed diffusion-weighted imaging for differentiating synovial proliferation from joint effusion in hand arthritis

Yuki Tanaka[1] · Motoshi Fujimori[1] · Koichi Murakami[2] · Hiroyuki Sugimori[3] · Nozomi Oki[4] · Takatoshi Aoki[5] · Tamotsu Kamishima[3]

Received: 29 June 2019 / Accepted: 10 August 2019 / Published online: 27 August 2019

Abstract

The objective of this study is to investigate computed DWI (cDWI) as an alternative method to contrast-enhanced MRI in comparison with directory measured DWI (mDWI) and apparent diffusion coefficient (ADC) for differentiating synovial proliferation from joint effusion. Nine patients suspected with RA (5 women) were included in this study. A radiologist identified region of interest (ROI) based on STIR, and evaluated using a 5-point grading scale of 0 (fluid) to 4 (synovial proliferation) according to the degree of contrast enhancement within the ROI. cDWI was synthesized for *b* values from 1000 to 2000 at 200 s/mm^2 intervals using the combination of *b* values at mDWI. In addition to ADC values, contrast ratios were calculated using signal intensity for each ROI on the mDWI and cDWI. Visual assessment by a radiologist was conducted between pairs of STIR image and mDWI or cDWI. ROI grades were most significantly correlated with $cDWI_{2000}$ based on *b* values of 400–1000 s/mm^2 ($r_s = 0.405$, $p < 0.01$). The area under the curve of $cDWI_{2000}$ based on *b* values of 400–1000 s/mm^2 (0.762) was larger than that of ADC values (0.570–0.608) when comparing low versus high contrast enhancement grades. Both $cDWI_{1800}$ (200–1000) and $cDWI_{2000}$ (400–1000) demonstrated high sensitivity and specificity in visual assessment (84.6% and 66.7%, respectively). The $cDWI_{2000}$ based on *b* values of 400–1000 s/mm^2 may be useful for noninvasive differentiation of synovial proliferation from joint effusion in hand arthritis.

Keywords Arthritis · Synovial proliferation · MRI · Computed diffusion-weighted imaging

Introduction

Synovium is the primary site of inflammation and a major effector organ in a variety of joint diseases, including rheumatoid arthritis (RA) [1]. Inflamed synovium and effusion should be regarded as two distinct entitles [2], and proliferative synovitis is the earliest pathologic abnormality in RA, and is also responsible for bone and cartilage damage [3]. MRI is a sensitive technique available to assess joint inflammation [4]. T1-weighted spin-echo sequence early after intravenous

✉ Tamotsu Kamishima
ktamotamo2@yahoo.co.jp

Yuki Tanaka
yuki-0214tnk@eis.hokudai.ac.jp

Motoshi Fujimori
fujimori@frontier.hokudai.ac.jp

Koichi Murakami
k.murakami@m-satellite.jp

Hiroyuki Sugimori
sugimori@hs.hokudai.ac.jp

Nozomi Oki
ohki.nozomi@gmail.com

Takatoshi Aoki
a-taka@med.uoeh-u.ac.jp

[1] Graduate School of Health Sciences, Hokkaido University, North-12 West-5, Kita-ku, Sapporo 060-0812, Japan

[2] AIC Yaesu Clinic, 2-1-18, Nihonbashi, Chuo-ku, Tokyo, Japan

[3] Faculty of Health Sciences, Hokkaido University, North-12 West-5, Kita-ku, Sapporo 060-0812, Japan

[4] Department of Radiological Sciences, Nagasaki University Graduate School of Biomedical Sciences, 1-7-1 Sakamoto, Nagasaki 852-8501, Japan

[5] Department of Radiology, School of Medicine, University of Occupational and Environmental Health, 1-1 Iseigaoka, Nishi-ku, Kitakyushu, Fukuoka 807-8555, Japan

contrast material administration helps in the differentiation of synovial inflammation from the joint effusion in RA; however, the technique is somewhat invasive due to the use of gadolinium contrast agents, which may cause severe adverse/side effects [5–8].

Diffusion-weighted imaging (DWI) presents a non-invasive approach to contrast-free imaging of synovitis in the hands of RA [9, 10]. Although synovial proliferation is often less bright on DWI as well as short tau inversion recovery (STIR) compared with joint effusion, these cannot be easily differentiated [6, 11]. As DWI is based on a T2-weighted sequence, the signal intensity in *b* value images does not only depend on the diffusivity of water molecules but also on the T2 relaxation properties of the tissue leading to T2 shine-through effect [12, 13]. High *b* value images can decrease the influence of the T2 shine-through; however, they may cause image distortion and weakening of the signal-to-noise ratio because the phase shift by the stronger diffusion gradient results in greater dephasing [14, 15]. Moreover, the longer time to echo for higher *b* value DWI decreases the MR signals [16].

Computed DWI (cDWI) is a recently developed technique in which non-measured DWI at higher *b* values can be mathematically derived from directly measured lower *b* value DWI using the apparent diffusion coefficient (ADC) without direct image acquisition [17]. The cDWI can be obtained without additional scanning and the distortion of the images in higher *b* value DWI, and has the potential to improve the lesion-to-background contrast ratio (CR) compared with directly acquired lower *b* value DWI [17–19].

We hypothesized that cDWI could be an alternative to contrast-enhanced MRI in the assessment of synovial proliferation in hand arthritis because synovial proliferation has high signal intensity and joint effusion has low signal intensity on both images. This point is decisively different from the use of ADC map in hand arthritis, and from other previous studies focusing on tumor which reduces the background signal around the lesion and improves the detection rate of the lesion [18, 20, 21]. The purposes of this study were, therefore, [1] to investigate whether cDWI could be an alternative method of contrast-enhanced MRI in comparison with directory measured DWI (mDWI) and ADC value, and [2] to determine the cDWI with optimal *b* value, and with optimal combination of lower *b* values for differentiating synovial proliferation from joint effusion in the hands of patients with arthritis.

Materials and methods

Patients

A total of nine patients (5 women and 4 men; median age 61 years; age range 26–74 years) who underwent MRI of the hands participated in this prospective study. All had pain and/or swelling of the hand indicative of RA; one satisfied the 2010 American Rheumatism Association criteria for RA; and eight patients were diagnosed as unclassified arthritis [22]. Informed consent was obtained from all patients, and this prospective study was approved by the local ethics committee of our institution.

MRI

All images were acquired using a 3.0-T whole body MR system (Ingenia Omega HP, Philips Medical Systems, Best, The Netherlands) with a 20-channel phased-array Head–Neck coil. Patients were set in a prone position with both arms extended over their heads. The examinations included coronal STIR, DWI, and post contrast-enhanced MRI for the hands.

STIR with the following parameters was utilized: TR/TE = 4076/50 ms, flip angle = 90°, field of view (FOV) = 240 mm × 240 mm, matrix size = 320 × 320 [480 × 480], number of slices = 25, slice thickness/gap = 2.0/0.2 mm, number of excitation (NEX) = 2, acquisition time (AT) = 1 min 37 s. The imaging parameters for spin-echo echo-planar DWI (SE-EPI-DWI) with SPIR (spectral presaturation with inversion recovery) were as follows: TR/TE = 5074–6098/83.9–87.2 ms, flip angle = 90°, FOV = 240 mm × 240 mm, matrix size = 128 × 128 [256 × 256], number of slices = 25, slice thickness/gap = 2.0/0.2 mm, EPI factor = 63, NEX = 2, *b* values = 0, 200, 400, 1000 s/mm^2, AT = 3 min 30 s. For contrast-enhanced MRI, 3D-T1 fast field echo sequence using modified DIXON with the following parameters was utilized: TR/TE = 6.01–6.18/1.39–2.5 ms, flip angle = 10°, FOV = 240 mm × 240 mm, matrix size = 192 × 192 [512 × 512], number of slices = 55, slice thickness = 2.0 mm, NEX = 1, and the contrast agent (0.1 ml/kg of body weight of gadobutrol; Gadovist, Bayer Schering Pharma, Berlin, Germany) was injected using an automatic MR compatible contrast injection device (Sonic Shot 7, Nemoto Kyorindo, Tokyo, Japan) at a rate of 3 ml/s at the time of the first acquisition phase following acquisition of a baseline dynamic scan. The number of phases and acquisition time per phase was 26 phases and 12.4 s. Data in brackets are imaging parameters after zero-filled interpolation (ZIP). ZIP is a technique to expand the image matrix size filling in the missing cells of k-space with zeroes [23], AT = 5 min 10 s.

Image analysis

Three ROIs were placed in three regions of each wrist (distal radioulnar, radiocarpal, and intercarpal–carpometacarpal joints) using an image viewer (EV Insite S; PSP, Tokyo, Japan). One radiologist (AA with 19 years of experience as

musculoskeletal radiologist), who was blinded to other clinical information, manually placed regions of interest (ROIs) in the suspected synovial proliferation or joint effusion on STIR. The suspected synovial proliferation or joint effusion was evaluated on contrast-enhanced MRI by three radiologists (AA, BB, and CC; BB and CC have 25 and 7 years of experience as musculoskeletal radiologist) using 5-point grading scale of 0 [no enhance: water (joint effusion)], 1 (1–25%), 2 (26–50%), 3 (51–75%) and 4 (76–100%: synovial proliferation) according to the degree of contrast enhancement (hereafter: contrast enhancement grade).

The cDWI signal for $b = b_c$ was obtained with the equation $S_c = S_1 \times \exp[-(b_c - b_1)\mathrm{ADC}]$. We generated cDWI with b value of 1000 s/mm^2 (cDWI_{1000}) from mDWI with b values of 0 and 200 (0–200), 0 and 400 (0–400), 200 and 400 (200–400) s/mm^2, and cDWI with b values of 1200, 1400, 1600, 1800, 2000 s/mm^2 ($\mathrm{cDWI}_{1200,1400,1600,1800,2000}$) from mDWI with b values of 0 and 200 (0–200), 0 and 400 (0–400), 200 and 400 (200–400), 0 and 1000 (0–1000), 200 and 1000 (200–1000), 400 and 1000 (400–1000) s/mm^2. One radiological technologist with 1 year of experience (DD) carefully placed the same ROI on mDWI_0 ($b = 0$ s/mm^2), while referring to the ROI position on STIR images, and then the ROI placement on mDWI_0 was copied and pasted on mDWI and cDWI images with each b value.

For quantitative analysis, we calculated contrast ratios (CRs) using signal intensity (SI) for each ROI on mDWI and cDWI. CRs were calculated as $\mathrm{CR} = \mathrm{SI}_{\mathrm{ROI}}/\mathrm{SI}_{\mathrm{muscle}}$, where $\mathrm{SI}_{\mathrm{ROI}}$ and $\mathrm{SI}_{\mathrm{muscle}}$ were the average SI for the ROI and right adductor pollicis muscle, respectively. Using mDWI signals, ADC value was calculated on the basis of a mono-exponential model with the formula: $\mathrm{ADC} = (-S_1/S_2)/(b_1 - b_2)$, where S_1 is SI for $b = b_1$ and S_2 is SI for $b = b_2$.

For qualitative analysis, visual assessment by a radiologist (AA) was conducted between pairs of STIR image and mDWI/cDWI [mDWI_{1000}, cDWI_{1600} (200–1000), cDWI_{1800} (200–1000), cDWI_{2000} (200–1000) and cDWI_{2000} (400–1000)]. The images were presented in random order to the observer, who was blinded to other clinical information except for the ROI location on STIR. The radiologist (AA) classified the SI of the ROI on DWIs compared to STIR as follows: presence of SI = 1, absence of SI = 0.

Statistical analysis

All statistical analyses were performed using the Statistical Package for the Social Sciences (SPSS) version 24.0 for Windows (IBM Corp., New York, NY, USA) and Excel (Microsoft Corp., Redmond, WA, USA).

Correlations between CRs of DWI/ADC values and contrast enhancement grades were assessed with Spearman's rank correlation test. If CRs of DWI and ADC values show significant correlation with contrast enhancement grade, receiver operating characteristic (ROC) curve analysis was performed to assess the ability to differentiate between joint effusion and synovial proliferation. For ROC analysis using quantitative (CRs of DWI and ADC values) and the qualitative (SI of the DWI) assessment, we defined grades 0, 1, and 2 as joint effusion and grades 3 and 4 as synovial proliferation. We calculated the area under the curve (AUC) for the quantitative assessment, and sensitivity, specificity, positive predictive value (PPV), and negative predictive value (NPV) for the qualitative assessment. In addition, we defined grade 0 as pure joint effusion and grade 4 as pure synovial proliferation for clear differentiation, and calculated the parameters concerning qualitative assessment. Interpretation of AUC is that a test with an area greater than 0.9 has high accuracy, while 0.7–0.9 indicates moderate accuracy, 0.5–0.7, low accuracy and 0.5 a chance result [24]. $P < 0.05$ was considered statistically significant.

Results

MRI datasets were successfully acquired from all nine patients (men, median age 61 years, age range 26–74 years; women, median age 54 years, age range 41–72 years). A total of 54 ROIs of suspected synovial proliferation and/or joint effusion were confirmed on STIR images from all patients. As for contrast-enhanced MRI, five ROIs were excluded due to the dual presence of both synovial proliferation and joint effusion. Therefore, we targeted 49 ROIs for DWIs and ADC values. The number of contrast enhancement grade for each ROIs was as follows: grade 0 ($n = 12$), 1 ($n = 13$), 2 ($n = 6$), 3 ($n = 5$), 4 ($n = 13$). Representative MR images for analysis of synovial proliferation and joint effusion are shown in Figs. 1 and 2.

Figure 3 shows the correlations between DWIs/ADCs and contrast enhancement grades. The cDWI of 11 image types had significant correlation with contrast enhancement grade (Table 1), that was most significantly correlated with cDWI_{2000} (400–1000) ($r_s = 0.405$, $p = 0.004$). As shown in Table 2, area under the curves (AUCs) of cDWI of 11 image types were larger than those of ADC values, and 9 image types of cDWI in these 11 image types indicated moderate accuracy in ROC analysis. Tables 3 and 4 showed the calculated parameters of qualitative assessment using mDWI_{1000} and cDWIs [cDWI_{1600} (200–1000), cDWI_{1800} (200–1000), cDWI_{2000} (200–1000), cDWI_{2000} (400–1000)] which showed high correlation with contrast enhancement grade. Qualitative assessment using 5-point grades targeted 49 ROIs, and using only grades 0 and 4 targeted 25 ROIs. Specificity, PPV and NPV of cDWI_{1800} (200–1000) and cDWI_{2000} (400–1000) were especially larger than that of mDWI_{1000} in the visual assessment using only grades 0 and 4.

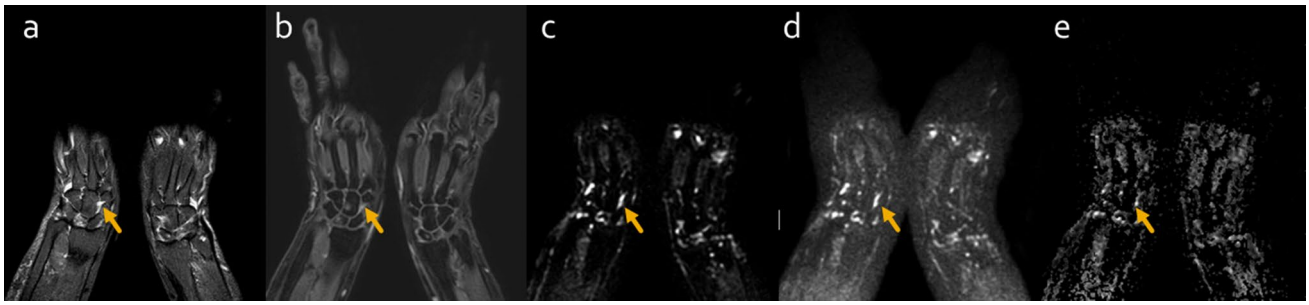

Fig. 1 A representative case with positive synovial proliferation. MR images in a 72-year-old woman with suspected rheumatoid arthritis. **a** STIR. **b** Contrast-enhanced MRI at the sixth phase (approximately 60 s after initiation of contrast injection). **c**, **d** DWI ($b = 400$ and 1000 s/mm^2). **e** Computed DWI with b value of 2000 s/mm^2 based on b values of 400–1000 s/mm^2. The ROI of suspected synovial proliferation and/or joint effusion in the intercarpal–carpometacarpal joint of the left hand (arrows) demonstrates high signal intensity on STIR and contrast-enhanced MRI (grade 4: contrast enhance of 75–100%). *MR* magnetic resonance, *STIR* short tau inversion recovery, *DWI* diffusion-weighted imaging, *ROI* region of interest

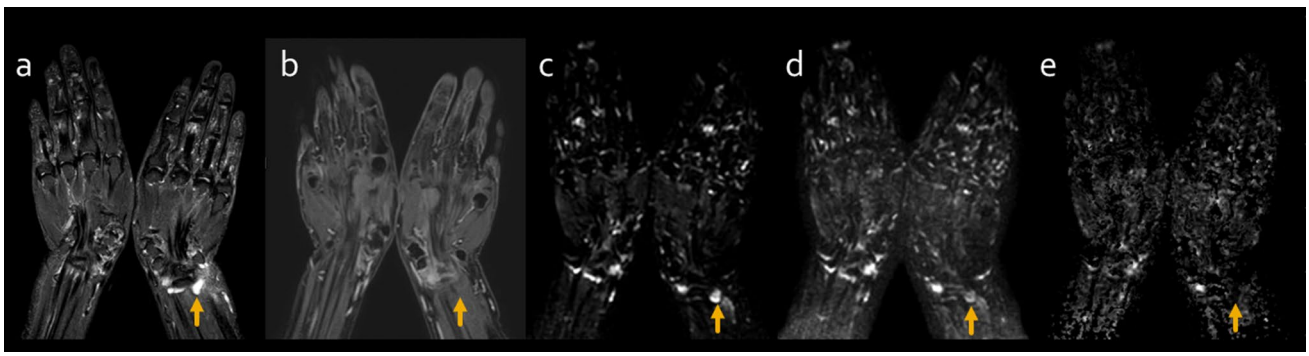

Fig. 2 A representative case with joint effusion. MR images in a 72-year-old woman with suspected rheumatoid arthritis. **a** STIR. **b** Contrast-enhanced MRI at the sixth phase (approximately 60 s after initiation of contrast injection). **c**, **d** DWI ($b = 400$ and 1000 s/mm^2). **e** Computed DWI with b value of 2000 s/mm^2 based on b values of 400–1000 s/mm^2. The ROI of suspected synovial proliferation and/or joint effusion in the radiocarpal joint of the right hand (arrows) demonstrates high signal intensity on STIR and low signal intensity on contrast-enhanced MRI (grade 0: no enhancement). *MR* magnetic resonance, *STIR* short tau inversion recovery, *DWI* diffusion-weighted imaging, *ROI* region of interest

Discussion

For differentiating synovial proliferation from joint effusion, cDWI with b value of 2000 s/mm^2 based on b values of 400 and 1000 s/mm^2 showed the potential as an alternative method to contrast-enhanced MRI in this study.

Detection of synovial proliferation is significant for early diagnosis in RA [25], and contrast-enhanced MRI has been conducted as definitive diagnosis for differentiating synovial proliferation from joint effusion. However, the injection of intravenous contrast increases medical cost, pain, and discomfort of patients [5–8]. In addition, some patients cannot receive a contrast medium because of their allergic reaction or impaired renal function. Therefore, non-contrast-enhanced MR sequence for detection of synovial proliferation has clinical advantages.

ADC is the slope of the line formed by the measured two signal intensities in the logarithmic scale, and is used for differentiating synovial proliferation from joint effusion in RA because of difference of diffusion coefficient [26]. ADC values, however, showed no significant difference between them in this study. This discrepancy might be derived from difference in the degree of inflammation within the ROI. Although we used a 5-point grading scale according to contrast enhancement, about half of contrast enhancement grades within ROI were determined as middle grades (grades 1, 2, 3). Since ADC is the slope utilizing signal intensity of ROI, it might be difficult to distinguish the slight differences between synovial proliferation and joint effusion, which show middle grades, using ADC values.

cDWI is a mathematical computation technique which synthesized DWI from two mDWIs with different b values

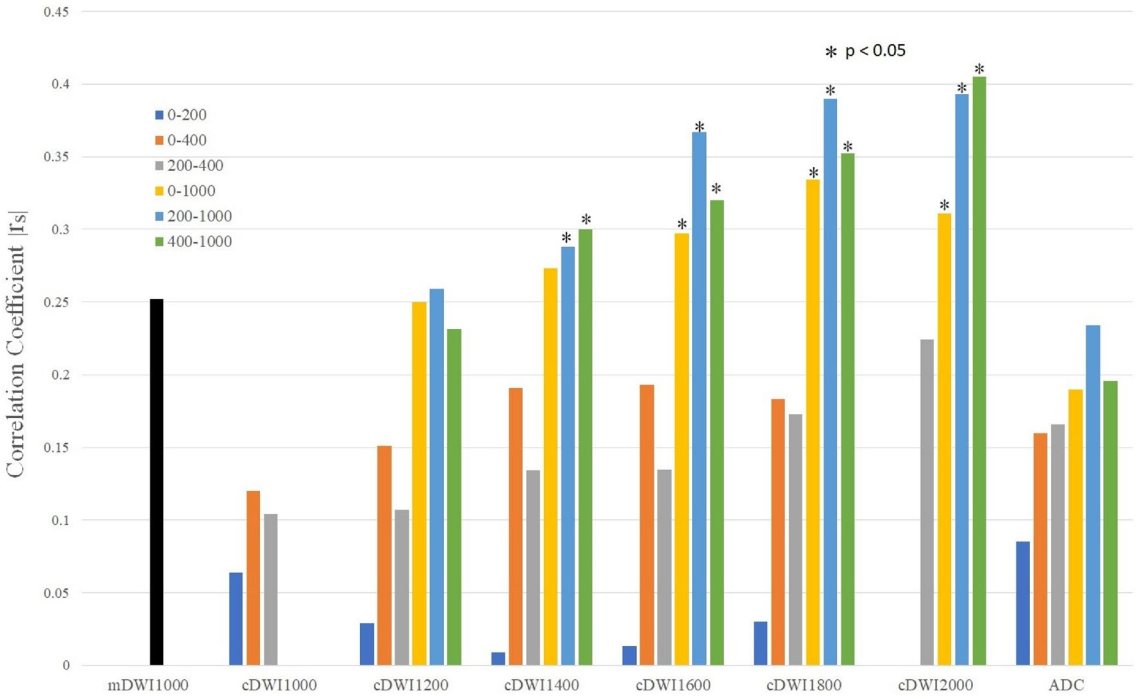

Fig. 3 Correlation coefficient between CRs of DWI and ADC values and contrast enhancement grades with Spearman's rank correlation test. *CR* contrast ratio, *DWI* diffusion-weighted imaging, *ADC* apparent diffusion coefficient, *mDWI* directly measured diffusion-weighted imaging, *cDWI* computed diffusion-weighted imaging

Table 1 Correlation coefficient of image types which showed significant correlation with contrast enhancement grades

Image type	Correlation coefficient
$cDWI_{1400}$ (200–1000)	0.288 ($p=0.044$)
$cDWI_{1400}$ (400–1000)	0.300 ($p=0.036$)
$cDWI_{1600}$ (0–1000)	0.297 ($p=0.038$)
$cDWI_{1600}$ (200–1000)	0.367 ($p=0.010$)
$cDWI_{1600}$ (400–1000)	0.320 ($p=0.025$)
$cDWI_{1800}$ (0–1000)	0.334 ($p=0.019$)
$cDWI_{1800}$ (200–1000)	0.390 ($p=0.006$)
$cDWI_{1800}$ (400–1000)	0.352 ($p=0.013$)
$cDWI_{2000}$ (0–1000)	0.311 ($p=0.030$)
$cDWI_{2000}$ (200–1000)	0.393 ($p=0.005$)
$cDWI_{2000}$ (400–1000)	0.405 ($p=0.004$)

Data in brackets of image type mean combination of *b* values for calculating cDWI [e.g., $cDWI_{2000}$ (400–1000) means cDWI with *b* value of 2000 s/mm^2 based on *b* values of 400 and 1000 s/mm^2]

cDWI computed diffusion-weighted imaging

and can reduce imaging acquisition time while producing images with a higher signal-to-noise ratio (SNR) than mDWIs. In ROC analysis, cDWI including mDWI with *b* values of 0, 200 or 400, and 1000 s/mm^2 tended to show better AUC than that including mDWI with low b values, and ADC values. The SI of ROI on cDWI decreases greatly when synthesizing cDWI with high *b* value using mDWI with low b values, which include not only diffusion in the slow component but also perfusion information in the fast component [27]. Our results showed that combination of *b* values with 400 and 1000 s/mm^2 was optimal for cDWI generation, and higher *b* value of cDWI had higher accuracy for distinction of synovial proliferation. A previously performed study concerning prostate cancer detection suggests that *b* value combinations with $b \geq 10$ and $b \geq 500$ s/mm^2, as well as $b=0$ and 1000 s/mm^2 are recommended for computation DWI at *b* value with 2000 s/mm^2 [28]. The previous study found that signals of relatively small cancers tend to be weaker on cDWI generated from *b* values <500 s/mm^2 because initial decrease in SI at low *b* values is steeper than the more gradual attenuation of SI at higher *b* value. Further, Fujimori et al. demonstrate that monoexponential model using mDWI with *b* value greater than 200 s/mm^2 rather than with *b* values of 0 and 1000 s/mm^2 is preferred for precise detection of synovial proliferation [29]. The result of the current study is consistent with these previous studies. Therefore, the combination of *b* values of 400 and 1000 s/mm^2 was optimal for differentiating synovial proliferation from joint effusion in this study.

In visual assessment, $cDWI_{1800}$ (200–1000) and $cDWI_{2000}$ (400–1000) had higher specificity, PPV and NPV than $mDWI_{1000}$. $mDWI_{1000}$ had only high sensitivity because the number of true positives and false positives increased due to not only synovial proliferation but also joint effusion

Table 2 Accuracy, sensitivity, and specificity of cDWI and ADC for differentiating contrast enhancement grades indicative of joint effusion vs those indicative of synovial proliferation in quantitative analysis

	AUC (95% CI)	*p* value	Cutoff value	Sensitivity (%)	Specificity (%)
$cDWI_{1400}$ (200–1000)	0.686 (0.529–0.844)	0.031	1.60	41.2	93.5
$cDWI_{1400}$ (400–1000)	0.715 (0.562–0.868)	0.013	1.61	41.2	93.5
$cDWI_{1600}$ (0–1000)	0.692 (0.528–0.856)	0.026	1.43	47.1	93.5
$cDWI_{1600}$ (200–1000)	0.720 (0.567–0.874)	0.011	1.19	64.7	71.0
$cDWI_{1600}$ (400–1000)	0.729 (0.575–0.884)	0.008	1.19	64.7	71.0
$cDWI_{1800}$ (0–1000)	0.729 (0.573–0.886)	0.008	1.08	70.6	74.2
$cDWI_{1800}$ (200–1000)	0.737 (0.586–0.887)	0.006	1.11	64.7	83.9
$cDWI_{1800}$ (400–1000)	0.746 (0.594–0.897)	0.004	1.02	82.4	67.7
$cDWI_{2000}$ (0–1000)	0.711 (0.545–0.878)	0.014	1.06	64.7	74.2
$cDWI_{2000}$ (200–1000)	0.729 (0.567–0.892)	0.008	1.02	70.6	80.6
$cDWI_{2000}$ (400–1000)	0.762 (0.607–0.916)	0.002	1.10	64.7	80.6
ADC (0–200)	0.582 (0.406–0.759)	0.340	2.15	67.7	64.7
ADC (0–400)	0.608 (0.434–0.781)	0.213	1.93	87.1	41.2
ADC (0–1000)	0.570 (0.407–0.733)	0.419	2.08	45.2	76.5
ADC (200–400)	0.608 (0.439–0.776)	0.213	2.32	48.4	76.5
ADC (200–1000)	0.600 (0.441–0.760)	0.245	1.90	51.6	76.5
ADC (400–1000)	0.575 (0.414–0.737)	0.384	1.80	45.2	82.4

Data in brackets of cDWI and ADC mean combination of *b* values for calculating cDWI and ADC [e.g., $cDWI_{2000}$ (400–1000) means cDWI with *b* value of 2000 s/mm^2 based on *b* values of 400 and 1000 s/mm^2]

cDWI computed diffusion-weighted imaging, *ADC* apparent diffusion coefficient, *AUC* area under the curve, *CI* confidence interval

Table 3 Sensitivity, specificity, PPV, and NPV of mDWI and cDWI for differentiating contrast enhancement grades indicative of joint effusion vs those indicative of synovial proliferation in qualitative analysis

Image type	Sensitivity (%)	Specificity (%)	PPV (%)	NPV (%)
$mDWI_{1000}$	94.4	9.68	37.8	75.0
$cDWI_{1600}$ (200–1000)	77.8	38.7	42.4	75.0
$cDWI_{1800}$ (200–1000)	72.2	41.9	41.9	72.2
$cDWI_{2000}$ (200–1000)	55.6	38.7	34.5	60.0
$cDWI_{2000}$ (400–1000)	72.2	45.2	43.3	73.7

Data in brackets of image type mean combination of *b* values for calculating cDWI [e.g., $cDWI_{2000}$ (400–1000) means cDWI with *b* value of 2000 s/mm^2 based on *b* values of 400 and 1000 s/mm^2]

mDWI directly measured diffusion-weighted imaging, *cDWI* computed diffusion-weighted imaging, *PPV* positive predictive value, *NPV* negative predictive value

Table 4 Sensitivity, specificity, PPV, and NPV of mDWI and cDWI for differentiating contrast enhancement grades indicative of joint effusion vs those indicative of synovial proliferation in qualitative analysis using only grades 0 and 4

Image type	Sensitivity (%)	Specificity (%)	PPV (%)	NPV (%)
$mDWI_{1000}$	92.3	16.7	54.5	66.7
$cDWI_{1600}$ (200–1000)	84.6	50.0	64.7	75.0
$cDWI_{1800}$ (200–1000)	84.6	66.7	73.3	80.0
$cDWI_{2000}$ (200–1000)	53.8	58.3	58.3	53.8
$cDWI_{2000}$ (400–1000)	84.6	66.7	73.3	80.0

Data in brackets of image type mean combination of *b* values for calculating cDWI [e.g., $cDWI_{2000}$ (400–1000) means cDWI with *b* value of 2000 s/mm^2 based on *b* values of 400 and 1000 s/mm^2]

mDWI directly measured diffusion-weighted imaging, *cDWI* computed diffusion-weighted imaging, *PPV* positive predictive value, *NPV* negative predictive value

by T2 shine-through effect showing high SI. In this study, visual assessment of cDWI could differentiate only the cases with pure synovial proliferation (grade 4) and pure joint effusion (grade 0). Further investigation of appropriate sequence parameters and future improvement of MRI technology might be possible to differentiate synovial proliferation from joint effusion irrespective of the degree of inflammation. cDWI exhibits high SI in synovial proliferation as with contrast-enhanced MRI, while ADC map exhibits low SI in that. Therefore, cDWI is preferred as an alternative method of contrast-enhanced MRI for the assessment of joint inflammation.

This prospective study had several limitations. First, we did not compare mDWI with *b* values greater than 1000 s/mm^2 with cDWI, because high *b* value mDWI, especially at the hands, may not be suitable for clinical application due to image distortion, weakening of the SNR and longer acquisition time. Second, synovial proliferation in RA occurs in finger as well as wrist joints; nevertheless, we targeted only wrist joints because the small lesion in finger joint on mDWI may disappear when synthesizing cDWI with higher *b* value. Finally, although cDWI with optimal *b* value based on optimal combination of *b* values demonstrated significant difference between synovial proliferation and joint effusion, the study population was relatively small. Therefore, further study might be required to confirm the detectability for small lesions including finger joints using a larger patient population.

In conclusion, cDWI with optimal *b* value based on optimal combination of *b* values indicated to detect the difference of synovial proliferation and joint effusion which cannot be differentiated by mDWI and ADC values. We found that cDWI with *b* value of 2000 s/mm^2 based on *b* values of 400 and 1000 s/mm^2 had potential of alternative method of contrast-enhanced MRI for differentiating synovial proliferation from joint effusion.

Author contributions YT: substantial contributions to the analysis of the data for the work; and drafting the work or revising it critically for important intellectual content; and final approval of the version to be published; and agreement to be accountable for all aspects of the work in ensuring that questions related to the accuracy or integrity of any part of the work are appropriately investigated and resolved. MF: substantial contributions to the design of the work, the acquisition, analysis, and interpretation of data for the work; and drafting the work or revising it critically for important intellectual content; and final approval of the version to be published; and agreement to be accountable for all aspects of the work in ensuring that questions related to the accuracy or integrity of any part of the work are appropriately investigated and resolved. KM: substantial contributions to the conception and design of the work; and drafting the work or revising it critically for important intellectual content; and final approval of the version to be published; and agreement to be accountable for all aspects of the work in ensuring that questions related to the accuracy or integrity of any part of the work are appropriately investigated and resolved. HS: substantial contributions to the conception and design of the work; and drafting the work or revising it critically for important intellectual content; and final approval of the version to be published; and agreement to be accountable for all aspects of the work in ensuring that questions related to the accuracy or integrity of any part of the work are appropriately investigated and resolved. NO: substantial contributions to the conception and design of the work; and drafting the work or revising it critically for important intellectual content; and final approval of the version to be published; and agreement to be accountable for all aspects of the work in ensuring that questions related to the accuracy or integrity of any part of the work are appropriately investigated and resolved. TA: substantial contributions to the conception and design of the work; and drafting the work or revising it critically for important intellectual content; and final approval of the version to be published; and agreement to be accountable for all aspects of the work in ensuring that questions related to the accuracy or integrity of any part of the work are appropriately investigated and resolved. TK: substantial contributions to the conception and design of the work; and drafting the work or revising it critically for important intellectual content; and final approval of the version to be published; and agreement to be accountable for all aspects of the work in ensuring that questions related to the accuracy or integrity of any part of the work are appropriately investigated and resolved.

Funding This work has no funding support.

Compliance with ethical standards

Conflict of interest The authors declare that they have no conflict of interest.

Informed consent Informed consent was waivered because of the retrospective study design.

Ethical approval All procedures performed in studies involving human participants were in accordance with the ethical standards of the institutional and/or national research committee and with the 1964 Helsinki declaration and its later amendments or comparable ethical standards.

References

1. Tak PP (2000) Analysis of synovial biopsy samples: opportunities and challenges. Ann Rheum Dis 59:929–930
2. Burke CJ, Alizai H, Beltran LS, Regatte RR (2019) MRI of synovitis and joint fluid. J Magn Reson Imaging 49:1512–1527
3. Boutry N, Morel M, Flipo RM, Demondion X, Cotten A (2007) Early rheumatoid arthritis: a review of MRI and sonographic findings. AJR Am J Roentgenol 189:1502–1509
4. Goupille P, Roulot B, Akoka S et al (2001) Magnetic resonance imaging: a valuable method for the detection of synovial inflammation in rheumatoid arthritis. J Rheumatol 28:35–40
5. Ostergaard M, Edmonds J, McQueen F et al (2005) An introduction to the EULAR-OMERACT rheumatoid arthritis MRI reference image atlas. Ann Rheum Dis 64(Suppl 1):i3–7
6. Ostergaard M, Conaghan PG, O'Connor P et al (2009) Reducing invasiveness, duration, and cost of magnetic resonance imaging in rheumatoid arthritis by omitting intravenous contrast injection—does it change the assessment of inflammatory and destructive joint changes by the OMERACT RAMRIS? J Rheumatol 36:1806–1810

7. Sadowski EA, Bennett LK, Chan MR et al (2007) Nephrogenic systemic fibrosis: risk factors and incidence estimation. Radiology 243:148–157
8. Grobner T (2006) Gadolinium—a specific trigger for the development of nephrogenic fibrosing dermopathy and nephrogenic systemic fibrosis? Nephrol Dial Transpl 21:1104–1108
9. Li X, Liu X, Du X, Ye Z (2014) Diffusion-weighted MR imaging for assessing synovitis of wrist and hand in patients with rheumatoid arthritis: a feasibility study. Magn Reson Imaging 32:350–353
10. Qu J, Lei X, Zhan Y, Li H, Zhang Y (2017) Assessing synovitis and bone erosion with apparent diffusion coefficient in early stage of rheumatoid arthritis. J Comput Assist Tomogr 41:833–838
11. Narvaez JA, Narvaez J, De Lama E, De Albert M (2010) MR imaging of early rheumatoid arthritis. Radiographics 30:143–163 **(discussion 163–165)**
12. Stejskal EO, Tanner JE (1965) Spin diffusion measurements: spin echoes in the presence of a time-dependent field gradient. J Chem Phys 42:288–292
13. Colagrande S, Belli G, Politi LS, Mannelli L, Pasquinelli F, Villari N (2008) The influence of diffusion- and relaxation-related factors on signal intensity: an introductive guide to magnetic resonance diffusion-weighted imaging studies. J Comput Assist Tomogr 32:463–474
14. Le Bihan D, Poupon C, Amadon A, Lethimonnier F (2006) Artifacts and pitfalls in diffusion MRI. J Magn Reson Imaging 24:478–488
15. Koh DM, Blackledge M, Padhani AR et al (2012) Whole-body diffusion-weighted MRI: tips, tricks, and pitfalls. AJR Am J Roentgenol 199:252–262
16. Ben-Amitay S, Jones DK, Assaf Y (2012) Motion correction and registration of high *b*-value diffusion weighted images. Magn Reson Med 67:1694–1702
17. Blackledge MD, Leach MO, Collins DJ, Koh DM (2011) Computed diffusion-weighted MR imaging may improve tumor detection. Radiology 261:573–581
18. Rosenkrantz AB, Chandarana H, Hindman N et al (2013) Computed diffusion-weighted imaging of the prostate at 3 T: impact on image quality and tumour detection. Eur Radiol 23:3170–3177
19. Gatidis S, Schmidt H, Martirosian P, Nikolaou K, Schwenzer NF (2016) Apparent diffusion coefficient-dependent voxelwise computed diffusion-weighted imaging: an approach for improving SNR and reducing T2 shine-through effects. J Magn Reson Imaging 43:824–832
20. Ueno Y, Takahashi S, Kitajima K et al (2013) Computed diffusion-weighted imaging using 3-T magnetic resonance imaging for prostate cancer diagnosis. Eur Radiol 23:3509–3516
21. Kawahara S, Isoda H, Fujimoto K et al (2016) Additional benefit of computed diffusion-weighted imaging for detection of hepatic metastases at 1.5T. Clin Imaging 40:481–485
22. Paul BJ, Kandy HI, Krishnan V (2017) Pre-rheumatoid arthritis and its prevention. Eur J Rheumatol 4:161–165
23. Du YP, Parker DL, Davis WL, Cao G (1994) Reduction of partial-volume artifacts with zero-filled interpolation in three-dimensional MR angiography. J Magn Reson Imaging 4:733–741
24. Swets JA (1988) Measuring the accuracy of diagnostic systems. Science 240:1285–1293
25. Carotti M, Galeazzi V, Catucci F et al (2018) Clinical utility of eco-color-power Doppler ultrasonography and contrast enhanced magnetic resonance imaging for interpretation and quantification of joint synovitis: a review. Acta Biomed 89:48–77
26. Shimizu H, Isoda H, Fujimoto K et al (2013) Comparison of acquired diffusion weighted imaging and computed diffusion weighted imaging for detection of hepatic metastases. Eur J Radiol 82:453–458
27. Niu J, Li W, Wang H et al (2017) Intravoxel incoherent motion diffusion-weighted imaging of bone marrow in patients with acute myeloid leukemia: a pilot study of prognostic value. J Magn Reson Imaging 46:476–482
28. Ueno Y, Takahashi S, Ohno Y et al (2015) Computed diffusion-weighted MRI for prostate cancer detection: the influence of the combinations of *b*-values. Br J Radiol 88:20140738
29. Fujimori M, Murakami K, Sugimori H et al (2019) Intravoxel incoherent motion MRI for discrimination of synovial proliferation in the hand arthritis: a prospective proof-of-concept study. J Magn Reson Imaging. https://doi.org/10.1002/jmri.26660